| Journal of Coastal Research | 15 | 1 | 1–14 | Royal Palm Beach, Florida | Winter 1999 |
|---|---|---|---|---|---|

# Ripple Migration and Sand Transport Under Quasi-Orthogonal Combined Flows on the Scotian Shelf

**C.L. Amos†, A.J. Bowen‡, D.A. Huntley††, J.T. Judge§, and M.Z. Li†**

†Geological Survey of Canada
Bedford Institute of Oceanography
P.O. Box 1006, Dartmouth
Nova Scotia B2Y 4A2, Canada

‡Department of Oceanography
Dalhousie University
Halifax, Nova Scotia
B3H 4J1, Canada

††Polytechnic Southwest
Drake Circus, Plymouth
Devon, U.K.

§MARTEC Limited
5670 Spring Garden Road
Halifax, Nova Scotia
B3J 1H6, Canada

**ABSTRACT**

AMOS, C.L.; BOWEN, A.J.; HUNTLEY, D.A.; JUDGE, J.T.; and LI, M.Z., 1999. Ripple migration and sand transport under quasi-orthogonal combined flows on the Scotian Shelf. *Journal of Coastal Research*, 15(1), 1–14. Royal Palm Beach (Florida), ISSN 0749-0208.

Bed state, ripple migration and bedform transport of fine sand ($D_{50}$ = 0.23 mm) were recorded with time-lapse photography for 12 days in 22 m of water on Sable Island Bank, the Scotian Shelf, Canada. Near-bed wave and steady flows were recorded and correlated with observed bed state and ripple migration. A well-defined threshold for the traction of fine sand under largely orthogonal combined flows is apparent in our data. It is defined by the expression $\Theta_{cb}' = [\Theta_w' + \Theta_c'] = 0.04$. The value is 20% less than the threshold criterion defined by GRANT and MADSEN (1979) for wave-dominant flows and extends it to the current dominant flow conditions when flows are orthogonal to each other. In addition, a threshold for saltation/suspension under combined flows is defined by the expression $\Theta_{cb}' = [\Theta_w' + 1.5\Theta_c'] = 0.17$. This threshold marks the onset of saltation and grain bypassing of ripple lee faces and approximates closely the *breakoff* Shields parameter ($\Theta_{br}' = 0.16$) of GRANT and MADSEN (1982). Bedform transport measurements are applicable only below this point; termed the *equilibrium range* by GRANT and MADSEN (1982). The sediment transport model SEDTRANS matched the duration and magnitude of sand transport over a wide range of conditions of combined flow. This was achieved by using the method of GRANT and MADSEN (1979), but minimizing the friction factor ($f_{cw}'$) to 0.006. This value equals the pure unidirectional flow drag coefficient of SOULSBY (1983).

**ADDITIONAL INDEX WORDS:** *Sand transfer, ripple migration, combined flows threshold.*

## INTRODUCTION

Literature reviews by GRASS (1981), BEIBOER (1984), SLEATH (1984), HODGINS *et al.* (1986), DYER (1986) and SROKOSZ (1987), and measurements by INMAN and BOWEN (1963), THORN (1979), WILLIS (1979), VINCENT *et al.* (1981, 1983), NEIDORODA *et al.* (1982), SOULSBY *et al.* (1983), PATTIARATCHI and COLLINS (1984), MOODY *et al.* (1987), YOO and O'CONNER (1987), SOUTHGATE (1987), SOULSBY (1997) and others, suggest that sand transport by steady flows is enhanced significantly by wave motion. This enhancement is manifested by a decrease in the apparent unidirectional threshold for grain motion (BAGNOLD, 1963; HAMMOND and COLLINS, 1976; AMOS *et al.*, 1988; ARNOTT and SOUTHARD, 1990), and increases in bed shear stress (GROSS *et al.*, 1994). In order to determine combined-flow sediment transport it is first important to define suitable threshold criteria for each transport phase. Presently, explicit solutions are available for the threshold of bedload transport. By contrast, thresholds for saltation/suspension and sheet flow under oscillatory, unidirectional flows, or combined flows are contradictory, as are measurements of sediment transport rates under combined flows (LAVELLE *et al.*, 1978; HEATHERSHAW, 1981; PATTIARATCHI and COLLINS, 1984; WIBERG *et al.*, 1994; CACCHIONE *et al.*, 1994).

Attempts have been made to measure sediment transport in regions subject to waves and currents, and to compare the measurements to predictions (LAVELLE *et al.*, 1978; HEATHERSHAW, 1981; LEES, 1983; PATTIARATCHI and COLLINS, 1984). These have been discussed by DYER (1986), BOWEN (1986) and HUNTLEY (1986), and summarized by HODGINS *et al.* (1986) who stated: "The central problem in applying any of the existing [sediment transport] models in Canadian waters is the lack of reliable hydrodynamic input data and *in situ* sediment transport measurements. The primary requirement is for a field experiment to measure boundary layer hydrodynamics, sedimentary environment and sediment motion." The objectives of this study, therefore, were to collect a field data set suitable to the examination of the threshold for different sediment transport regimes in fine sand (median diameter $D_{50}$ = 0.23 mm), and to evaluate the use of current ripple migration as an index of bedload transport under combined flows.

*97051 received 21 July 1997; accepted in revision 18 October 1997.*

## THE MODEL

A computer model (SEDTRANS) was developed to calculate sediment transport under unidirectional and combined flows. The details of the model structure, coding and operation are given in Martec Ltd. (1982, 1983), DAVIDSON (1984), DAVIDSON AND AMOS (1985), Martec Ltd. (1986, 1987), AMOS AND JUDGE (1991), LI AND AMOS (1995), and LI AND AMOS (1997). SEDTRANS reproduced test results reported in GRANT AND GLENN, (1983) to within ± 3%. It comprises five subroutines which are reviewed below.

(1) Maximum near-bed wave orbital velocity ($U_b$) and maximum orbital diameter ($d_o$) are computed using standard linear wave theory:

$$U_b = \pi H_s/(T \sinh(kd)) \quad (1)$$

$$\text{and} \quad d_o = H_s/\sinh(kd). \quad (2)$$

Input parameters are significant wave height ($H_s$), water depth (d), and wave period (T). Linear wave theory is most applicable for small amplitude waves (H/L < 1/20). Conditions during the RALPH deployment were within this ratio (1/100 < H/L < 1/50, where L is the wave period). GRACE (1976) showed that linear wave theory is invalid under breaking waves, so the onset of this condition is evaluated with MICHE's (1994) equation before proceeding:

$$H_b = 0.142L \tanh(kd) \quad (3)$$

where $H_b$ is the breaker height, L is the wavelength, and k is the wave number determined iteratively from the linear wave theory dispersion equation:

$$\omega^2 = gk \tanh(kd) \quad (4)$$

and $\omega$ is the wave angular frequency ($2\pi/T$).

(2) The bottom friction factors ($f_c$, $f_w$, $f_{cw}$) and bed shear stresses ($\tau_b$, $\tau_w$) are computed. Under steady flows, a constant friction factor ($f_c$) = $6.0 \times 10^{-3}$ ($f_c/2 = c_d$, the total drag coefficient) is used following STERNBERG (1972), DYER (1980) and SOULSBY (1983, which was derived from field measurements over a flat sandy bed). Bed stress is derived from the quadratic stress law:

$$\tau_c' = 6.0 \times 10^{-3}/2\rho U_1|U_1| \quad (5)$$

where $U_1$ is the mean flow measured 1 m above the bed, and where ′ denotes the skin friction component. The friction factor (skin friction component) for pure wave motion ($f_w'$) is calculated using NIELSEN's (1979) modification of the JONSSON (1966) method:

$$f_w' = \exp[5.213(K_b'/A_b)^{0.194} - 5.977] \quad \text{for } A_b/K_b' > 1.7 \quad (6)$$

$$f_w' = 0.28 \quad \text{for } A_b/K_b' < 1.7. \quad (7)$$

$A_b$ is the maximum wave orbital amplitude ($d_o/2 = U_bT/2\pi$), and $K_b' = D_{50}$ (the grain roughness height). The velocity profile outside the wave boundary layer, as well as the total bed shear stress is determined using $K_b$, the physical roughness height, which is set to a value of 0.02 m based on VAN RIJN's (1982) relationship:

$$K_b = 1.1\eta[1 - \exp(-2\pi\eta/\lambda)] \quad (8)$$

where $\eta$ is ripple height, and $\lambda$ is ripple wavelength. A constant value was used as we had no direct measures of ripple height or steepness to warrant a more complicated form of $K_b$. The instantaneous velocity vector ($U(t) = U_b \cos \omega t$) is used with the quadratic stress law to derive bed stress ($\tau_w'$). Under combined flow conditions, an iterative procedure is necessary to stimulate the more complex form of friction factor ($f_{cw}'$). The partitioned components of the wave and steady current bed stresses are derived with the method of GRANT and MADSEN (1979). That is, the wave-enhanced mean bed shear stress ($\tau_c'$) is:

$$\tau_c' = \rho f_{cw}'(V_2/U)|U_b|^2 \quad (9)$$

and the maximum, combined wave/steady current bed shear stress is:

$$\tau_{cw}' = \rho f_{cw}'(\alpha/2)|U_b|^2 \quad (10)$$

$V_2$ and $\alpha$ are factors that account for the relative magnitudes of the steady and oscillatory currents at the top of the wave boundary layer, and the angle between them averaged over a wave cycle.

$\tau_{cw}'$ is checked against the equivalent bed shear stress determined using a steady flow drag coefficient. If the Grant and Madsen method predicts values of stress lower than the steady flow case, then the friction factor, $f_{cw}'$, is adjusted to equate both stress values. This is based on the assumption that the bed shear stress for a constant steady flow cannot decrease by the superposition of waves (GRANT and MADSEN, 1978).

(3) The threshold stresses for initiation of bedload transport and suspension are calculated. For steady flows, the bedload threshold velocity ($U_{cb}$) is derived from MILLER *et al.* (1977), and the saltation/suspension threshold velocity ($U_s$) is derived from BAGNOLD (1966). Under wave dominant conditions, the traction and sheet flow thresholds are derived from KOMAR and MILLER (1975) and the saltation/suspension threshold follows NIELSEN (1986). The critical combined flow Shields parameter ($\Theta_{cw}'$) for bedload transport is defined as:

$$\theta_{cw}' = \tau_{cw}'/(\Delta\rho g D_{50}) = 0.04 \quad (11)$$

where $\Delta\rho g$ is the buoyant weight of sediment ($\rho_s - \rho_f$)g. The threshold for pure unidirectional flows evaluated 1 m above the seabed ($U_1$) is 0.22 m/sec, and for pure oscillatory flow ($U_{cb}$) is about 0.17 m/sec.

These values correspond well to the threshold values reported by KOMAR (1976), KOMAR and MILLER (1975) and WHEATCROFT (1994). Equation 11 is valid under conditions of mixed flow over fine sand when the Reynolds number ($Re_* = U_*D_{50}/\upsilon$, where $\upsilon$ is the fluid kinematic viscosity and $U_*$ is the friction velocity) is greater than 10. The BAGNOLD (1966) saltation/suspension threshold Shields parameter ($\Theta_{cs}'$) is used for all conditions of flow as it is dependent only on fluid density ($\rho_f$) and particle settling rate ($W_s$):

$$\theta_{cs}' = 0.64\rho_f W_s^2/(\Delta\rho g D_{50}) = 0.12 \quad (12)$$

$W_s$ is equated with the upward instantaneous velocity component of flow which is approximately equal to 0.8 times the friction velocity ($v_{up}' = 0.8U_*$); it is calculated using GIBBS *et al.* (1971). Assuming spherical grains 0.23 mm in diameter,

a water temperature of 10°C, and a sediment density of 2,650 kg/m$^3$, $W_s$ = 0.026 m/sec. It is important to note that the threshold for motion of poorly sorted sediments is different from that of well-sorted ones (SAMAGA *et al.*, 1986). Sediments in this study were well sorted ($\sigma < 1.0$).

(4) The timing of each transport mode over a wave cycle is particularly important for conditions of combined flow, and provides the limits of integration for estimating sediment transport over a wave cycle. For oscillatory flow it involves the solution of the following equations:

$$|U_b \cos \omega t| = U_{cb} \quad \text{for bedload,} \tag{13}$$

$$\text{or} \quad |U_b \cos \omega t| = U_{cs} \quad \text{for suspended load.} \tag{14}$$

$U_{cb}$ and $U_{cs}$ (the threshold velocities defined 1 m above the bed) were derived from equations 11 and 12 respectively after solving for the appropriate skin friction factors using equations 6 or 7. The combined wave and current case is more complex. In this case, $U_{cb}$ and $U_{cs}$ are based on a skin friction factor that is modified according to GRANT and MADSEN (*ibid*). To determine the duration of sediment transport, the magnitude of the instantaneous (total) velocity vector is equated to the respective critical velocities in the following quadratic equations:

$$\cos \omega t = -|U_b|^{-1}\left[|U_a| \cos \varphi_b \pm (U_{cb}^2 - |U_a|^2 \sin^2 \varphi_b)^{1/2}\right] \tag{15}$$

$$\cos \omega t = -|U_b|^{-1}\left[|U_a| \cos \varphi_b \pm (U_{cs}^2 - |U_a|^2 \sin^2 \varphi_b)^{1/2}\right] \tag{16}$$

where $U_a$ is the steady current velocity at the top of the wave boundary layer used in the bottom stress calculations, and $\varphi_b$ is the angle between the wave and current directions inside the wave boundary layer. No phase lag is assumed between onset of stress and sediment response. Earlier, GRANT and MADSEN (1982) showed that grain response is $O(10^{-1})$ sec. The last set of terms in equations 15 and 16 are added for $0 < t < \pi$ (wave crest), and subtracted for $\pi < t < 2\pi$ (wave trough).

(5) The wave-averaged net sediment transport ($Q_s$) is determined in the presence of a mean current. Instantaneous dry weight sediment discharge was computed using the (EINSTEIN)-BROWN (1950) bedload equation as used by MADSEN and GRANT (1976):

$$Q_s = 40\gamma W_s D_{50}\left[|\tau_{cw}'|/((\rho_s - \rho_f)gD_{50})\right]^3 \text{ kg/m/sec} \tag{17}$$

where $\gamma$ is the sand bulk density (1,800 kg/m$^3$, after TERZAGHI and PECK, 1967). Wave-averaged sediment discharge is determined by integrating $Q_s$ between the thresholds of sediment transport over a wave cycle, and then dividing by the wave period (T). The equation is based on flume experiments on well-sorted sediment ranging in size from 0.3 to 29 mm, and so is untested for the grain size of this study. It was calibrated against the data of GILBERT (1914) who measured bedload as all transported material (so it includes saltation). The method is valid only for Shields parameters in excess of 0.09 which is slightly above the traction threshold. It produced good results for GRANT and MADSEN (1979) when the skin friction component only was used in the computation of bed stress. Nevertheless, the calibration data set used by MADSEN and GRANT (*ibid*) was for purely oscillatory conditions, not combined flows.

The effect of sediment transport on the friction factor is not considered. Under conditions of sheet flow, this effect could increase $f_{cw}'$ to $O(10^{-1})$ or greater (CACCHIONE *et al.* 1987; WIBERG and NELSON, 1992). Because we are dealing mainly with bedload transport this omission is assumed to be reasonable.

## Site Description

The data used in this study was collected in 22 m of water, on the crest of a sand ridge located southeast of Sable Island on Sable Island Bank (Lat. 44-02-06N; Long. 59-33-44W; Figure 1). The site was near the Venture hydrocarbon discovery sites, for which the geology, oceanography, climatology and biology are known (Mobil Oil Canada Ltd., 1983). The seabed, at the time of data collection, was composed of well-sorted, fine quartzose sand ($D_{50}$ = 0.23 mm) molded into wave- and current-formed ripples (AMOS *et al.*, 1988a). The site is subject to the influences of tidal currents which peak at 0.35 m/sec, storm-driven currents which peak at 0.76 m/sec, and waves which have a 50-year peak period of 12 seconds and a 50-year characteristic wave height of 14 m. Consequently, the site experiences a wide range of steady and oscillatory, near-bed flows.

## Methodology

### Instrument Package

The data for this study were collected by a microprocessor-controlled, free standing instrument package—RALPH—described by HEFFLER (1984). The package consisted of a Sea Tech Inc. transmissometer mounted 1.5 m above the bed, a Marsh-McBirney electromagnetic current meter (model 512 OEM) mounted 1.0 m above the bed that recorded two orthogonal components of flow, an upward-looking sonar and pressure transducer mounted 2.0 m above the bed, and a downward-looking Minolta XL401, super-8 camera and synchronised 50 J flash. The nodal line of the camera was set 20° from nadir, to produce a field of view approximately 1.0 × 1.5 m. The sensitivity, accuracy and limits of detection of the sensors are given in HEFFLER (1984).

### Sampling Strategy

The sampling strategy, data quality and data transformations of the RALPH deployment are described in detail by AMOS *et al.* (1988a). The instrument burst-sampled all channels for 512 seconds at 1 Hz each 2 hours. Every noon, the full burst-sampled time-series was stored; at all other times, the mean values and mean deviations only were stored. Two successive, time-lapse photographs of the seabed were taken each 30 minutes; the first under conditions of ambient light, and the second with a flash. At noon each day, a series of 50 photographs were taken at intervals of 8 seconds (corresponding with the burst-sampling of the instrument). The current meter and transmissometer performed well throughout the deployment. The pressure sensor, on the other hand, failed 6 days into the experiment, however, the upward-looking sonar showed significant interference from air bubbles in the water

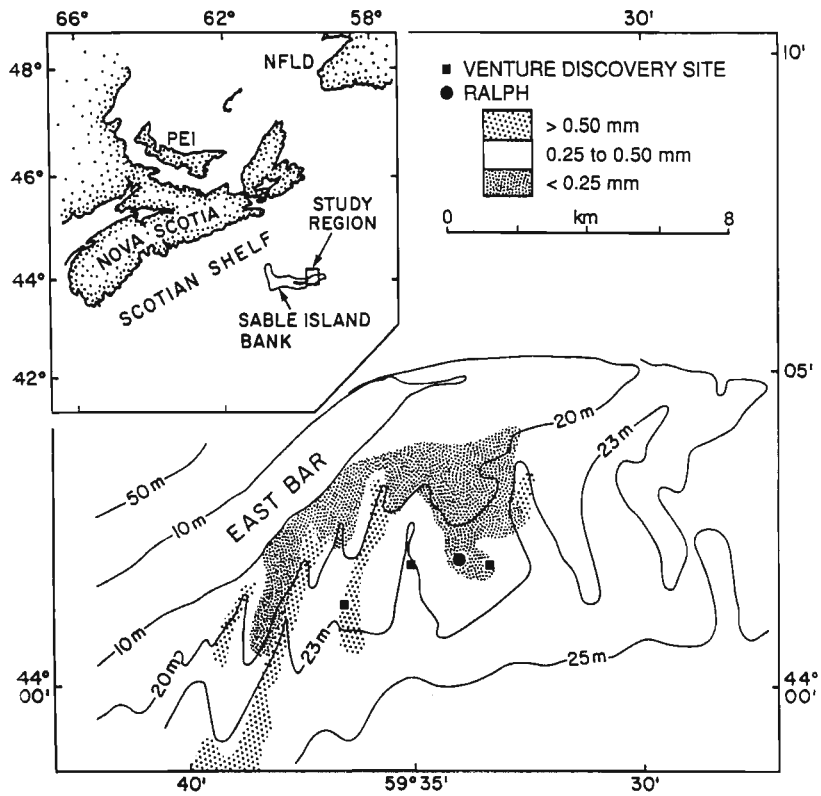


Figure 1. A location diagram of the experiment site on Sable Island Bank, Scotian Shelf, Canada.

column. Consequently, smoothing of the data was necessary in order to derive surface wave heights.

### Burst-Sampled Time-Series

Burst-sampled time-series were transformed based on specifications given by HEFFLER (1984). Mean surface wave period (T) was determined from a zero-crossing analysis from the noon-time burst data from the upward-looking sonar. Wave direction ($DIR_w$) was determined from the amplitude of the two measured oscillating flow components ($\dot{U}_x$ and $\dot{U}_y$) following the removal of the time-averaged mean current: $\dot{U}_x(t) = (U_x(t) - \overline{U}_x)\dot{U}_y(t) = (U_y(t) - \overline{U}_y(t))$; and $DIR_w = \tan^{-1}(\dot{U}_x(t)/\dot{U}_y(t))$. A review of the burst-sampled results for this deployment is given in AMOS *et al.* (1987, 1988).

### Mean Values

LONGUET-HIGGINS (1952) demonstrated that for random surface waves a correlation exists between significant wave height ($H_s$), the rms wave amplitude ($a_{rms}$) and the mean deviation of this amplitude ($a_{md}$). Transformation of $a_{md}$ to $H_s$ is, therefore, possible. GUZA and THORNTON (1980) confirmed the relationship: $H_s = 4a_{rms}$. So, assuming Gaussian processes:

$$a_s = 1.25a_{md} \text{ (SPIEGEL, 1961)}, \quad (18)$$

$$\text{and} \quad H_s = 5.0a_{md}. \quad (19)$$

This thoretical relationship, though valid for a narrow wave spectrum only, was used to derive $H_s$ from the bi-hourly measures of $a_{md}$. Bi-hourly wave period was derived by linear interpolation between burst-sampled data sets. The direction of wave propagation is known only for the burst series. It was assumed to be constant for each 24-hour interval between bursts due to small changes in measured wave direction from burst to burst. Wave direction varied between 270 and 305° only. Errors in direction brought about by the linear extrapolation are therefore less than 15°.

### Bedform Transport and Bedform Migration Rates

The migration rates of small-scale ripples are used to estimate sediment transport rate and direction under waves and currents. Bedform transport rate is derived directly from current ripple migration ($d_r$) per unit time (t) and the direction of bedform transport is assumed to be normal to the local ripple crestline orientation.

The classification of ripple types is based on methods described by AMOS *et al.* (1988a). Current ripples were present at the bed even under conditions of high wave activity. The migration rate of current ripples was determined by mapping three crestline positions at near-real scale from frame-to-frame in the time-lapse photography. Migration rates in excess of 1 mm/sec could result in aliasing of our data. This did not happen as migration rates varied systematically about

zero (in response to tidal flow) with maxima less than 0.19 mm/sec.

BAGNOLD (1941) and later YANG (1986) argued that large-scale bedforms (sand waves and dunes) and possibly ripples, migrate in proportion to the total load of sand transported, not just the bedload. To avoid possible ambiguities, the term *bedform transport rate* is used hereafter as the index of sediment motion. Under conditions where sediment is not intermittently suspended or does not by-pass ripples, the rates of bedform transport and bedload transport are by definition equal. The impact of these assumptions is discussed fully by HUNTLEY *et al.* (1991). The transformation of ripple migration rate to bedform transport rate has generally been derived in two ways which differ by a factor of two. ALLEN (1970), RUBIN and MCCULLOCH (1980), LANGHORNE (1981, 1982) and VAN DEN BERG (1987) propose the relationship:

$$Q_s = 1/2\eta(d_r/t)\rho_b \quad (20)$$

where $\eta$ is ripple height and $\rho_b$ is sediment bulk density. That is, the transported volume is equivalent to the ripple volume (per unit width) when $d_r = \lambda$, the ripple wavelength. BAGNOLD (1941) and later KACHEL and STERNBERG (1971) and YANG (1986) propose the relationship:

$$Q_s = \eta(d_r/t)\rho_b. \quad (21)$$

They argue that sand transport is equivalent to the trapezoid defined by the prograding ripple face through time ($\eta d_r$). BAGNOLD's (1941) sand transport term is defined at the ripple brink point only, and varies linearly in proportion to elevation with respect to the brink point (p. 204). Mean transport, over the bedform as a whole is thus proportional to mean bedform height, which (assuming tabular ripple faces) is $\eta/2$. Viewed simply, the two methods yield respectively the mean and maximum transport rates: we chose to use the mean value. Implicit in both methods is the assumption that ripple shape and size remain uniform.

$\eta$ was not measured in this study, but was inferred from a relationship to wavelength presented by ALLEN (1970) for current-formed ripples

$$\eta = 0.074\lambda^{1.19} \text{ (in cgs units) for } 0.04 \text{ m} < \lambda < 0.60 \text{ m}. \quad (22)$$

This approach differs from AMOS *et al.* (1988b) where a constant ripple height and wavelength were assumed. Implicit in equation 22 is that ripple steepness is related directly to wavelength; an assumption applicable within the equilibrium range only (GRANT and MADSEN, 1982). The mean ripple wavelength was 0.23 (± 0.06) m, and the calculated mean ripple height was, therefore, 0.03 (± 0.01) m. Volume was transformed to dry mass of sediment by assuming a bulk density and sediment density of 1,800 and 2,600 kg/m$^3$ respectively (after TERZAGHI and PECK, 1967). VAN DEN BERG (1987) quotes a wide range of observations which indicate sediment by-passing of ripples to be up to 40 to 60% of the total bedload at high current speeds. Thus, only 40% of the total load may have contributed to ripple migration. As a starting point, we chose to assume no by-passing. Sediment saltation and by-passing of ripples is seen (as blurring of photo images) at peak flows (LARSEN *et al.*, 1981). This was clear only at high flows, so it may have been missed at initial stages of saltation leading to an over-estimation of the saltation/suspension threshold.

## RESULTS

### The Deployment

RALPH was deployed on Sable Island Bank at 1413 local time (GMT + 3 hours) on June 29, 1982 (day 181). The site was in 22 m of water on the southern flank of East Bar, Sable Island in the trough of a shoreface-connected ridge (Figure 1). Bottom samples collected at the deployment site were composed of well-sorted, quartzose, fine to medium size sand ($D_{50}$ = 0.23 mm). Sidescan sonograms at the experiment site were featureless. The site was characterized by a strongly-aligned semi-diurnal tidal ellipse the semi-major axis of which trended NNE to SSW. Waves propagated NW in a quadrant between 270 and 300° (true) due to restrictions in fetch caused by Sable Island. Thus sand transport took place under conditions where oscillatory and steady flows were orthogonal (± 10°).

### The Data

Good quality oceanographic data were recorded from the time of deployment until approximately 1200, July 14, 1982: a record length of approximately 15 days. The camera provided photographs until 0700, July 11, 1982 (day 193). Thus 12 days of concurrent seabed and hydrodynamic observations were obtained, covering a neap-spring-neap cycle (Figure 2). The near-bed current was dominated by strong semi-diurnal flows reaching up to 0.35 m/sec (Figure 2B, solid dots). Two periods of moderate winds (greater than 7 m/sec) and relatively high wave activity ($1.0 < H_s < 1.5$ m) were detected, separated by periods of low wave activity. Mean wave period varied between 8 and 10 sec. Near-bed mean amplitude of oscillatory flows ($U_{md}$) was greatest on days 182 and 186 ($75 < U_{md} < 150$ mm/sec; Figure 2B, open dots). The latter part of the experiment was relatively wave-free. A total of 139 measures of bedform transport and associated wave conditions and mean currents were made.

### Bed States, Thresholds and Ripple Migration Rates

The bed state changed rapidly with changing oceanic conditions during the course of the measurements. These states, discussed in AMOS *et al.* (1988a) corresponded to no motion, traction (with small scale ripples), saltation/suspension (transitional to upper plane bed), and sheet flow over plane bed. When steady flows dominated, the greatest current ripple migration rate ($d_r/t \approx 9.7 \times 10^{-2}$ mm/sec) and bedform transport rate ($3.7 \times 10^{-5} < i_s < 6.0 \times 10^{-3}$ kg/m/sec; Figure 2C) corresponded closely with peaks in tidal flow, but showed significant wave contributions. This is clear on day 186 when wave enhancement of neap tidal flows resulted in high ripple migration and bedform transport.

Figure 3 shows interpreted current-formed ripple migration rates plotted in terms of the mean and oscillatory currents. The scatter in the data was typically a factor of two of the mean. Nevertheless, bed state shows a good segregation between no motion (plane bed; ✘), transitional or intermit-

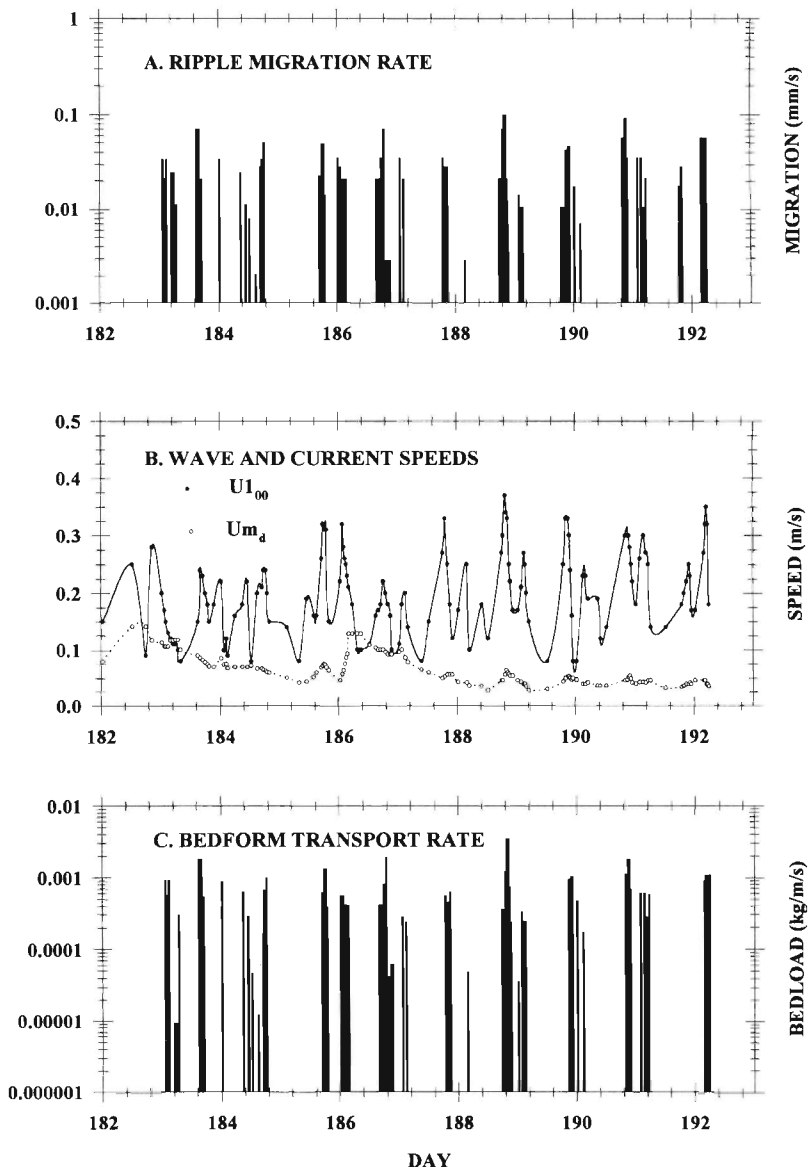


Figure 2. Time series of the (a) ripple migration rate, (b) near-bed mean current speed ($U_{100}$) and near-bed current mean deviation ($U_{md}$), and (c) bedform transport rate, for the duration of the RALPH deployment on Sable Island Bank. The figure shows strong, semi-diurnal tidal currents superimposed by two periods of high, near-bed wave motion. Sand transport is periodic and corresponds to peaks in the tidal flow.

tent transport (poorly-developed ripples; Δ) and measurable bedform migration (well-developed ripples; O) with little scatter in the data. The threshold for traction by unidirectional currents is significantly reduced (from 0.22 m/sec to <0.1 m/sec) by the presence of an oscillatory flow ($U_{md} < 0.04$ m/sec) and is near zero for $U_{md} > 0.04$ m/sec. The traction threshold and the threshold for ripple generation appear as two separate curves in Figure 3 (annotated as $10^{-4}$ and $10^{-3}$ mm/sec respectively). The triangles represent conditions when ripples are poorly developed; that is, ripple destruction is almost equal to the rate of formation by steady flows (AMOS *et al.*, 1988a). Under these conditions, sediment movement takes place without ripple generation, due to bioturbation. As bioturbation is seasonal, there is a practical and site-specific lower limit of applicability of the ripple migration rate as an index of sediment transport that is time variable. WHEATCROFT (1994, his Figure 9) found a similar situation on the northern California Shelf suggesting that this effect may be typical of continental shelves. The extent to which waves augment bedform transport is evident in Figure 3. The contours of ripple migration rate show trends which vary with $U_1$ and $U_{md}$. The peak in the ripple migration rate is interpreted to fall on a locus (solid line in Figure 3) defined by the least squares, best fit relationship:

$$U_{md} + 3U_1^3 \approx 0.13 \text{ m/sec } (r^2 = 0.99). \quad (23)$$

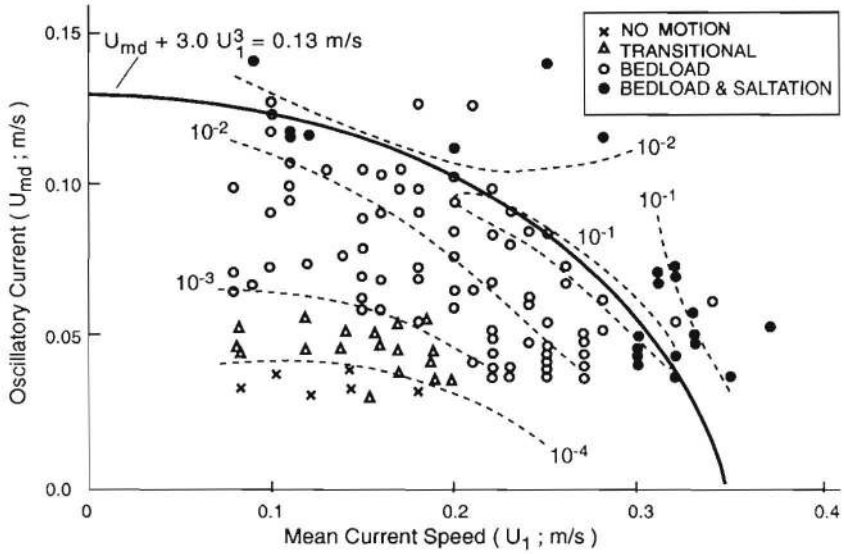


Figure 3. Smoothed current-formed ripple migration rate (dashed curves, mm/sec) plotted in terms of the mean current ($U_1$; m/sec) and mean deviation of the oscillatory, wave-induced current ($U_{md}$; m/sec). There is a segregation between conditions of no motion (X), intermittent motion (Δ) and continuous motion (O). Ripple breakoff (solid curve) is defined by the locus $U_{md} + 3\ U_1^3 = 0.13$ m/sec. This also defines the threshold for saltation/suspension (solid circles). The decrease in ripple migration rate beyond the breakoff line reflects an increase in ripple by-passing of the saltating grains.

Also, visual observations of saltation and ripple bypassing (●) were detected for cases only beyond the locus defined by equation 23. This locus is interpreted to be the breakoff region described by GRANT and MADSEN (1982) for wave-formed ripples. This is because below the locus (the so-called equilibrium range), ripple migration rate increases with flow, and a constant ripple steepness may be assumed; above the breakoff region, ripple migration rate may either increase or decrease and ripples degrade. The breakoff region, according to GRANT and MADSEN (1982), represents a transition between "high" and "low" sediment transport rates. Our data shows that it marks the onset of saltation and intermittent suspension—the saltation/suspension threshold. This is supported by the detailed observations of VINCENT and DOWNING (1994, their Figure 8) who showed that the suspended sand concentration increased markedly at the breakoff point.

When $U_{mb} < 0.04$ m/sec, ripple migration rate ($d_r/t$) increases with steady current speed, to a maximum of $U_1 = 0.33$ m/sec with no evidence of breakoff. The rate of ripple migration is approximated in terms of the excess current speed:

$$d_r = 4 \times 10^{-5} \exp(0.46(U_1 - U_{cb})). \quad (24)$$

STERNBERG (1967), who measured ripple migration under unidirectional tidal flow, derived the relationship:

$$d_r = (1.45 \times 10^{-10} \text{ to } 12.6 \times 10^{-10})U^5. \quad (25)$$

Our results, even at low oscillatory speeds ($U_{md} < 0.030$ m/sec), show a higher rate of increase in ripple migration than observed by Sternberg. This suggests that oscillatory flows influence significantly the migration rate of current-formed ripples, even when no evidence of waves is manifested in the ripple morphology.

At intermediate values of $U_{md}$ (0.05 to 0.10 m/sec), migration rates are greater and show a more complex relationship with mean flow. When $U_{md} > 0.13$ m/sec, current-formed ripple migration rate *decreases* as mean flow increases. The explanation for this decrease is given later and is attributed to a transition from equilibrium to transitional bed states. When $U_{md} > 0.13$ m/sec, the peak in ripple migration rate is at $U_1 < 0.05$ m/sec. Under such wave conditions, saltation/suspension occurs at virtually all mean flows with a resulting lack of correlation between flow and ripple migration rate. It follows that bedform migration rates above the breakoff region are poor indices of sediment transport. Thus, conditions during which ripple migration rate was strongly related to mean flow prevailed for 30% of the RALPH deployment only.

## Steady Current Direction and Ripple Orientation

AMOS *et al.* (1988a) showed that wave-formed and current-formed ripples are oriented with the directions of wave propagation and mean flow irrespective of the superposition of these flows. This may present a problem when waves and currents form oblique angles to each other because we define observed bedform transport to be in the direction of the current-formed ripple propagation. Yet, under such conditions, according to the Grant and Madsen method, the net sediment transport direction would vary significantly from that of the mean flow. The divergence of ripple orientation from the direction of the mean bed shear stress direction could lead to an under-estimation of the prevailing bedload transport rate by up to cos(30°) or about 15%. Under such circumstances, would the direction of net sediment transport be oblique to the axis of the current-formed ripples? Alternatively, would the current-formed ripples be aligned with the net sediment

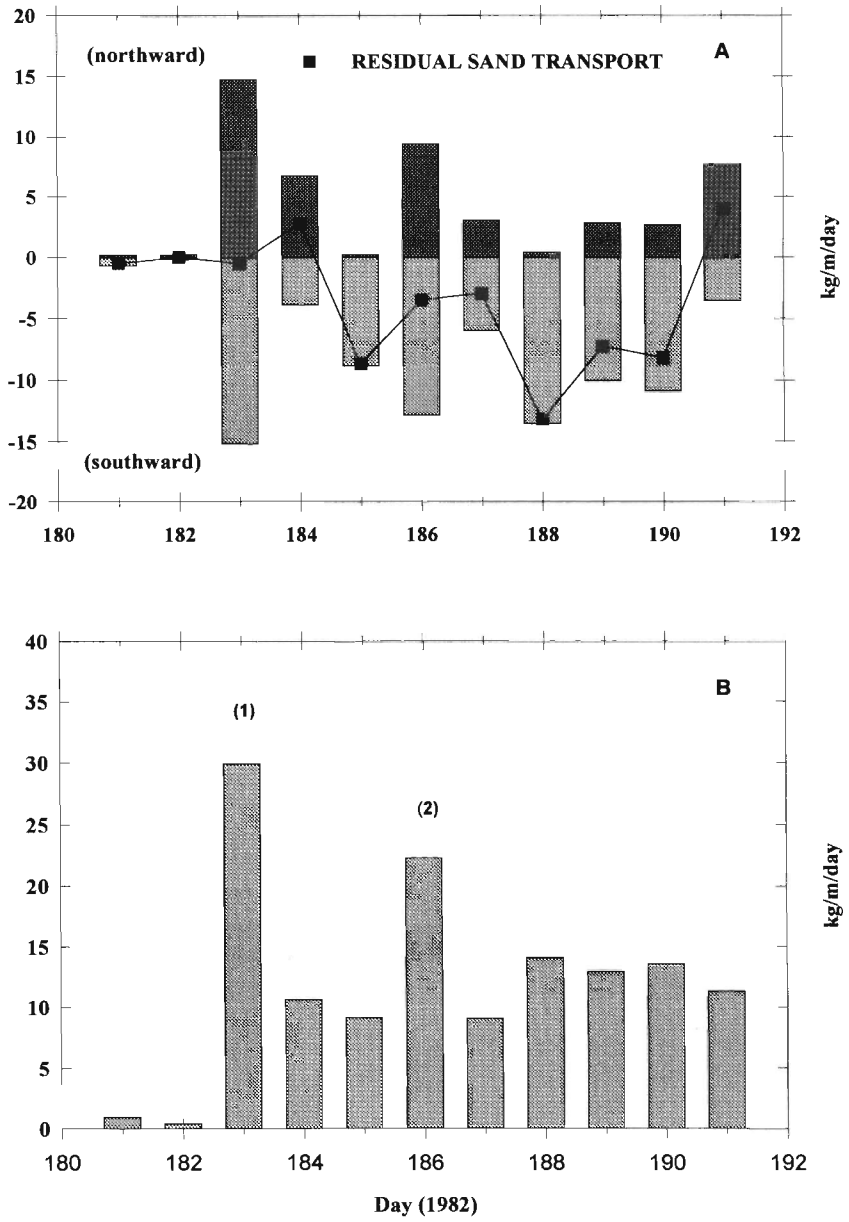


Figure 4. (a) The net bedform transport (kg/m) measured during this study. Note the peaks in transport during the two storms, and during spring (peak) tidal flow. Storm 1 took place during neap tides and reflects the strong influence of oscillatory flow on sand transport. (b) The absolute daily bedform transport (kg/m) for the duration of the RALPH deployment. The influence of oscillatory flows during the two storms has a significant effect on the net sand transport rate.

transport direction, and thus be oblique to the mean current? Our results, derived from orthogonal combined flows, showed a reasonable agreement between the directions of mean tidal flow and observed ripple migration ($r^2 = 0.61$). Though maximum differences in direction were approximately 30%, systematic deviations could not be attributed to high wave activity. So it seems that current ripples migrate in the direction of mean flow when wave enhancement is normal to this direction. What takes place when waves are oblique to steady currents is still uknown.

## Net Bedform Transport Rates

Net and total bedform discharges are shown in Figures 4A and 4B respectively. Transport was to the south(west) at an average rate of 5.9 kg/m/day. The cumulative NNE and SSW bedform transport during the experiment was 42 kg/m and 100 kg/m respectively. The daily residual transport was nearly zero during neap tides (days 181 (30 June)–184 (3 July)) and greatest during spring tides, when peak tidal currents were greatest (day 188 (7 July); Figure 4A). The two peaks

in near-bed wave motion (storms 1 and 2) had no obvious effect on the residual transport but increased significantly the total transport (Figure 4B). Even during storms, the total transport was small compared to the 480 kg/m/day measured by radio-isotope detection near this site during winter months (HODGINS, DRAPEAU and KING, 1986). It is also significantly less than net rates measured elsewhere by LAVELLE *et al.* (1978; 27 kg/m/day), HEATHERSHAW (1981; 267 kg/m/day), LEES (1983; 146 kg/m/day) and PATTIARATCHI and COLLINS (1984; 544 kg/m/day). These studies used tracer detection methods, and so results include the effects of traction, suspension and general dispersion. Our results are, however, comparable to ripple migration measurements made by STERNBERG (1967; $3 \times 10^{-2}$ mm/sec), KACHEL and STERNBERG (1971; 0.2–2.2 $\times 10^{-1}$ mm/sec) and BOYD *et al.* (1988; 0–2.7 $\times 10^{-2}$ mm/sec). It appears, therefore, that the sand transport magnitudes measured in this study are typical of tidal settings free from wave influences, but are not representative of long-term conditions of an exposed, storm-dominated continental shelf.

## THRESHOLDS FOR SAND MOTION: THEORY VERSUS OBSERVATION

Three thresholds of sand transport (traction, saltation/suspension, and sheet flow) are defined in terms of equivalent Shields parameters. Under unidirectional flow, the traction threshold is re-evaluated using YALIN (1977) for sea water at 10°C:

$$\Theta_{cb}' = f(\Delta\rho g D_{50}^3/\rho\nu^2)^{0.5} = \rho U_*'/(\Delta\rho g D_{50}) = 0.05 \quad (26)$$

where $U_*'$ is the friction velocity (skin friction component). Equation 26 defines the incipient motion of bed sediment and the development of a rippled bed (absent of bioturbation). Yalin's method eliminates the friction velocity term in the abscissa of the Shields diagram and accounts for variations in sediment density and temperature effects on sea water viscosity. This is important on the Scotian Shelf, where water temperatures may be 15–20°C lower than laboratory waters upon which much of the threshold data is based.

The Shields parameter for the onset of saltation/suspension under steady currents (equation 12) is 0.12, and for the threshold for sheet flow is defined by BAGNOLD (1966):

$$\theta_{css}' = C_o \tan \alpha_o = 0.58 \quad (27)$$

where $\alpha_o$ approximates to the internal friction angle ($\tan \alpha = 0.963$, after ALLEN and LEEDER, 1980) and $C_o$ is a static volume concentration (1-porosity) defined by BAGNOLD (1966) as $0.6 < C_o < 0.7$. Insofar as this threshold defines an upper plane bed state, the drag is imparted exclusively through shear (skin friction; DYER, 1980).

Incipient motion under purely oscillatory flow has been defined by KOMAR and MILLER (1974) in terms of the ratio of nearbed wave orbital diameter ($d_o$ to grain diameter (for $D_{50} < 0.5$ mm):

$$\rho U_b^2/(\Delta\rho g D_{50}) = 0.21\,(d_o/D_{50})^{0.5}. \quad (28)$$

Equation 28 is transformed to a Shields parameter ($\theta_{wb}'$) by multiplying throughout by a wave friction factor ($f_w'$) as $f_w'\rho_f U_m^2 = \rho U_*^2$. Thus

$$\theta_{wb}' = 0.10 f_w'(d_o/D_{50})^{0.5} = 0.05. \quad (29)$$

This threshold is based on data derived from laboratory flume experiments on flat beds. The threshold is valid for turbulent smooth boundary layers only, which roughly corresponds to a maximum bed grain diameter of 0.5 mm. Associated mean wave conditions during this study were: mean wave height = 1.0 m; mean period = 9 seconds; water depth = 22 m. The resulting orbital diameter ($d_o$) was 0.59 m resulting in $(d_o/D_{50})^{0.5} = 51$. This ratio is beyond values reported in KOMAR and MILLER (1975) and may be outside the limits of applicability of equation 28. Nevertheless, using equation 6 (for $A_b/K_b' = 1{,}261$), $f_w' = 0.0093$ which results in the following pure wave Shields parameter for entrainment:

$$\theta_{wb}' = 0.001\,(d_o/D_{50})^{0.5} = 0.05. \quad (30)$$

The solution is equal to that for pure unidirectional flow (equation 26) and falls well within the scatter of the original data (KOMAR and MILLER, 1974). If a larger grain roughness is used ($2.5D_{50}$; see NIELSEN, 1992 for a review) then $\theta_{wb}' = 0.04$, which is 20% smaller than the unidirectional equivalent, but is equivalent to the value that fits the observations in this data set.

The threshold for saltation under waves ($\theta_{ws}'$) was determined using data from NIELSEN (1986). His figure 3 shows a universal relationship between the reference concentration ($C_o$) and dimensionless bed stress that is applicable to both flat and rippled beds, wherein as $C_o$ approaches O ($1.5 \times 10^{-4}$) kg/m$^3$, $\theta_r$ approaches 0.5 (where $\theta_r = \theta_{ws}'/(1 - \pi\eta/\lambda)^2$. That is, the sediment concentration within the saltation layer (as defined after EVERTS, 1973) approaches the limits of detection of sediment motion. Equating this lower limit to the erosion threshold, we arrive at the following saltation Shields parameter:

$$\theta_{ws}' = 0.5(1 - \pi\eta/\lambda)^2 = 0.17. \quad (31)$$

The threshold for suspension and sheet flow was taken from KOMAR and MILLER (1975):

$$\theta_{wss}' = 0.413 D_{50}^{-0.4} = 0.74. \quad (32)$$

Equation 32 is valid only when $D_{50}$ is defined in mm. It is largely based on warm water (20°C) flume tests in fine to coarse sand. The Shields parameter used to derive the coefficients in equation 32 is determined using grain diameter for bed roughness and so is independent of form drag.

The observation of a breakoff region in ripple migration rate is significant in this study as: (1) it denotes the onset of saltation/suspension of the bed sediment; and (2) it defines the limits within which ripple migration rates are reasonable indices of sediment (bedload) transport. Saltation under orthogonal flows thus occurs when $U_{md} + 3U_1^3 > 0.13$ m/sec. But does this threshold correspond with published threshold values? Figure 5 shows the bed states for our experiment plotted with published thresholds. The bed states recognised are: (1) plane bed (no motion); (2) rippled bed (bedload); and (3) rippled with evidence for by-passing (saltation/suspension). The thresholds for traction and sheet flow are shown

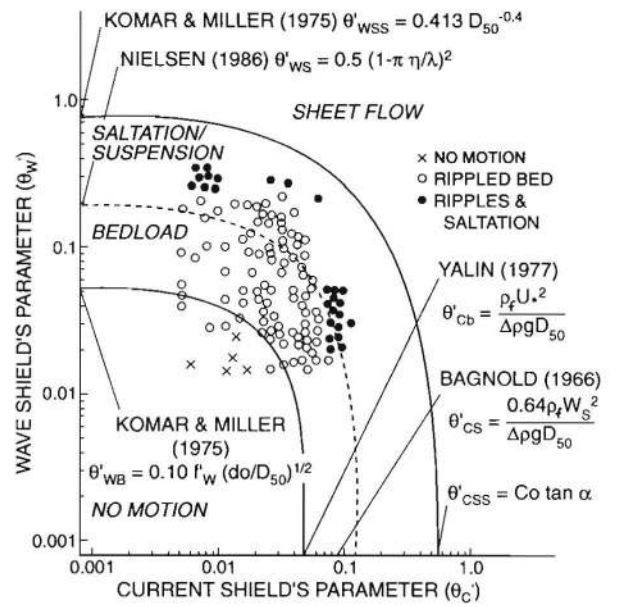


Figure 5. The partitioned wave and current Shields parameters for 139 observations of bed state recognised in the RALPH time-series. Bed states are defined as plane bed (no motion; X), rippled bed (bedload transport; O) and saltation/suspension (•), based on seabed time-lapse photography (Amos *et al.* 1988a). The traction and suspension thresholds for combined flows are plotted as the solid and dashed curves respectively. The superscript in the Shields parameter denotes a stress associated with skin friction only. The equations used to define the thresholds for the three phases of transport as well as for the onset of sheet flow are shown in the figure. Our data fits these thresholds quite well. Note the absence of results in the saltation/suspension to sheet flow transition.

by the solid curves, and the altation/suspension threshold by the dashed curve. The thresholds are straight lines on a linear plot and join the pure wave and pure current solutions. Note that our data indicates that the threshold for bedload transport is about 20% lower than predicted, however, the predicted threshold for saltation/suspension fits the data well. The combined flow traction threshold under orthogonal (or parallel) flows is shown by our data to be represented by the empirical expression:

$$[\Theta_w' + \Theta_c']_{crit.bed} = 0.04 \quad (33)$$

where $\Theta_w'$ and $\Theta_c'$ are the partitioned forms of the wave and steady-current Shields parameters respectively as defined in AMOS *et al.* (1988a). That is, $\Theta_w'$ includes the effect of the non-linear coupling of the combined flows, whereas $\Theta_c'$ does not. MADSEN and GRANT (1976) and later field observations of LARSEN *et al.* (1981) showed the correspondence between unidirectional and wave-induced thresholds provided the wave-induced bed stress was derived following the Madsen and Grant method. The $S_*$ parameter of MADSEN and GRANT (their Figure 5) was herein evaluated at 2.6 and the equivalent Shields parameter was 0.05.

In Figure 5 we see that the observed results on combined-flow, saltation/suspension threshold for orthogonal (or parallel) flows is approximated by the expression:

$$[\Theta_w' + 1.5\Theta_c']_{crit.susp} = 0.17. \quad (34)$$

This implies that mean bed shear stresses are more effective in causing saltation than oscillatory ones. This is unexpected in light of descriptions on vortex shedding off symmetrical ripples by WIBERG and NELSON (1992) and VINCENT and DOWNING (1994). This may be due to the ballistic action of saltating particles in ejecting more particles from the bed (LEEDER, 1979), which according to BAGNOLD (1941) takes time to build up and so would be better developed under unidirectional flows.

GRANT and MADSEN (1992) proposed that the Shields parameter at the ripple breakoff ($\Theta_{br}'$) is a function of the traction threshold and their dimensionless grain parameter ($S_*$):

$$\Theta_{br}' = 1.8S_*^{-0.6}\Theta_c' \quad (35)$$

$$\text{and} \quad S_* = (D_{50}/4\nu)[(\rho_s - \rho)gD_{50}]^{0.5}. \quad (36)$$

For a $D_{50}$ of 0.23 mm and $S_* = 2.6$, $\Theta_{br}' = 0.16$. This value is close to the combined flow threshold given in equation 34, and suggests that ripple breakoff begins at or close to the saltation threshold as suggested earlier. SAMAGA *et al.* (1986) proposed that under unidirectional flow there exists a fixed, critical ratio of friction velocity ($U_*$) to settling velocity ($W_s$) such that when $U_*/W_s > 0.5$ saltation/suspension of sand takes place. Our results indicate that this ratio is low, and that a better threshold ratio is that of BAGNOLD (1966; $U_*/W_s > 0.8$).

## An Evaluation of SEDTRANS

A comparison is made between the observed bedform transport and predictions made using (a) the combined bed shear stresses of GRANT and MADSEN (1979; Figure 6A), and (b) using GRANT and MADSEN (1979) with $f_{cw}'$ prevented from falling below 0.006 (Figure 6B). Figure 6A clearly shows an under-prediction in the duration and magnitude of sand transport. The cause of the under-prediction is the excessively low values of $f_{cw}'$ generated through the GRANT and MADSEN (1979) method under conditions of strong unidirectional flow i.e. the method is applied outside its range of application. Even under conditions of strong wave motion the method under-predicts between 20–40% (MADSEN and GRANT, 1976; their Figure 9). By minimizing $f_{cw}'$ to the pure unidirectional equivalent, determined by SOULSBY (1983) to be 0.006, SEDTRANS yields a better fit to the observations (Figure 6B). Even so, the fit is poor at early stages in the time-series (days 181–183) as conditions of strongest wave activity ($U_{md} > 0.9$ m/sec) and low mean tidal flow ($U_1 < 0.25$ m/sec) were prevalent. The poor correspondence is largely due to the absence of migrating ripples due to a weak mean flow; under such conditions sand transport is equated with the bioturbation rate (AMOS *et al.*, 1988b). For the remainder of the deployment the correspondence is good with the exception of a few isolated peaks in transport. These inconsistencies may result from observations being made beyond the breakoff region. This leaves the equilibrium range only where ripple migration may be correlated to sediment transport with any degree of confidence.

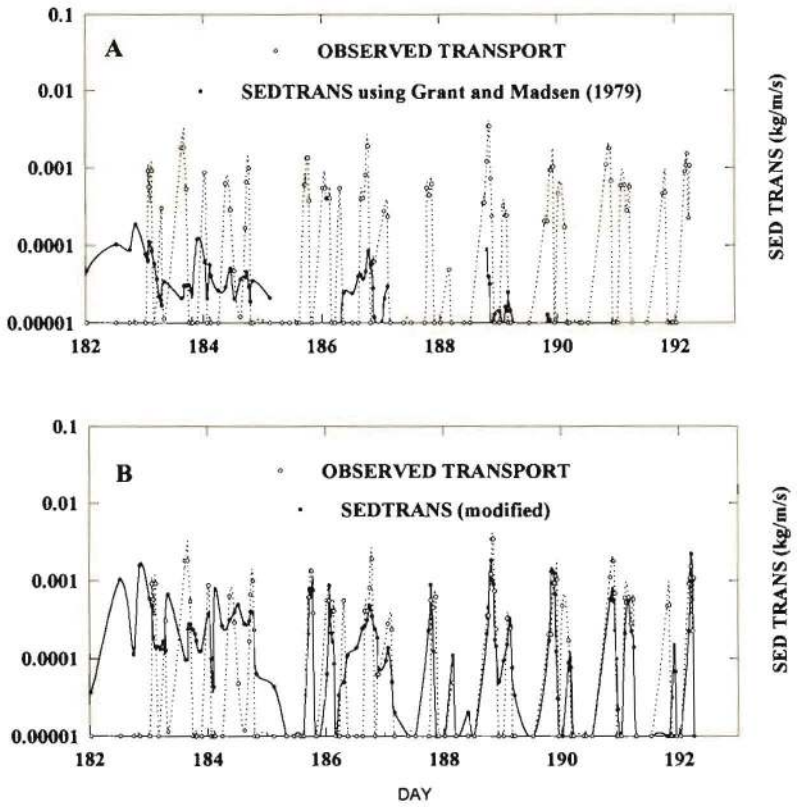


Figure 6. A time-series of observed bedform transport for the duration of the RALPH deployment plotted with predictions using SEDTRANS for (a) sediment transport based on the original Grant and Madsen (1979) method, and (b) minimizing $f_{cw}'$ to 0.006.

## CONCLUSIONS

Bedform transport of fine sand (0.23 mm) was measured under conditions of combined wave and tidal current motion, for purposes of comparison with published methods for computing bed shear stress and associated sediment transport. A number of conclusions are reached regarding the thresholds for traction and saltation/suspension, on the influences of waves on tidal flow induced sediment transport, and on the limits of application of ripple migration as an index of sand transport. The following are these conclusions:

(1) Net measured bedform transport for the duration of the experiment was to the southwest (5.9 kg/m/day). Maxima in transport (30 and 23 kg/m/day) took place during two storms. This illustrates the importance of storms on sediment movement at this site.
(2) Current ripple migration rate showed a good relationship to mean flow when wave oscillations near the bed were low ($U_{md} < 0.04$ m/sec).
(3) Ripple migration rate was a complex function of steady flow magnitude under combined flows. It increased to a maximum (the breakoff point) and then decreased. This is due to an increase in sediment by-passing at high flows due to saltation of sand.
(4) The critical traction threshold of fine sand is significantly affected by oscillatory flows, even when $U_{md} < 0.04$ m/sec. As waves and steady flows were largely orthogonal in this study, the observed combined flow traction threshold may be approximated by $(\Theta_w' + \Theta_c') = 0.04$.
(5) A combined-flow threshold for saltation/suspension is apparent from the observations. This threshold is well represented by data from BAGNOLD (1966) and NIELSEN (1986) at the pure current and pure wave limits and takes the form $(\Theta_{ws}' + 1.5\Theta_{cs}') = 0.17$ for orthogonal flows. This threshold matches the breakoff point for ripples predicted by GRANT and MADSEN (1982).
(6) Bedform transport, evaluated using the combined bed shear stress method of GRANT and MADSEN (1979), is underpredicted in both magnitude and direction. We feel that this is due in part to the application of the method beyond its range of applicability (to conditions dominated by steady flows). A closer agreement between SEDTRANS predictions and observations is obtained by minimizing the combined flow bed shear stress to that produced using $f_{cw}' = 0.006$ (Soulsby, 1983).

## ACKNOWLEDGEMENTS

This data set was the result of the efforts of C.F.M. Lewis and D.E. Heffler in co-operation with Mobil Oil Canada Ltd. and Canadian Hydrographic Service. The manuscript was reviewed by P. Hill, D.L. Forbes and R.W. Arnott. Funding for

data processing was made available from Environmental Studies Revolving Funds and the Offshore Geotechnics Program 63204 of the Federal Government of Canada Panel on Energy Research and Development. Geological Survey of Canada Contribution Number 36688.

## LITERATURE CITED


ALLEN, J.R.L., 1970. *Physical Processes and Sedimentation.* London: Unwin University books, 248p.

ALLEN, J.R.L. and LEEDER, M.R., 1980. Criteria for the instability of upper-stage plane beds. *Sedimentology,* 27, 209–217.

AMOS, C.L.; BOWEN, A.J.; HUNTLEY, D.A., and LEWIS, C.F.M., 1988a. Ripple generation under the combined influences of waves and currents on the Canadian continental shelf. *Continental Shelf Research,* 8(10), 1129–1153.

AMOS, C.L.; BOWEN, A.J.; HUNTLEY, D.A., and JUDGE, J.T., 1988b. Bedform stability under waves and currents. *Proceedings of Workshop on Friction Factors.* (Toronto, Ontario). Ottawa: Publication of the National Research Council of Canada, pp. 61–74.

AMOS, C.L. and JUDGE, J.T., 1991. Sediment transport on the eastern Canadian continental shelf. *Continental Shelf Research,* 11(8-10), 1037–1068.

ARNOTT, R.W. and SOUTHARD, J.B., 1990. Exploratory flow-duct experiments on combined-flow bed configurations and some implications for interpreting storm-event stratification. *Sedimentology,* 60(2), 211–219.

BAGNOLD, R.A., 1941. *The Physics of Blown Sand and Desert Dunes.* London: Chapman and Hall, 265p.

BAGNOLD, R.A., 1963. Mechanics of marine sedimentation. *In:* HILL, M.H., (ed.), *The Sea.* New York: Wiley-Interscience, pp. 507–582.

BAGNOLD, R.A., 1966. An approach to the sediment transport problem from general physics. *U.S. Geological Survey Professional Paper 4421,* 37p.

BEIBOER, F.L., 1984. Storm wave and current interaction. *Journal Society of Underwater Technology,* 10, 21–27.

BOWEN, A.J., 1986. Numeric modelling of sediment transport. *In:* HODGINS, D.O. (ed.), *Bottom Sediment Transport–Present Knowledge and Industry Needs.* Ottawa: Environmental Studies Revolving Funds Report 027, pp. 245–293.

BROWN, C.B., 1950. *Engineering Hydraulics.* ROUSE, H. (ed.). New York: Wiley, 1039p.

CACCHIONE, D.A.; DRAKE, D.E.; FERREIRA, J.T.; and TATE, B., 1994. Bottom stress estimates and sand transport on northern California inner continental shelf. *Continental Shelf Research,* 14, 1273–1289.

CACCHIONE, D.A.; GRANT, W.D.; DRAKE, D.E., and GLENN, S.M., 1987. Storm-dominated bottom boundary layer dynamics on the northern California continental shelf: Measurements and predictions. *Journal Geophysical Research,* 92, 1817–1827.

DAVIDSON, S., 1984. SED1D: a sediment transport model for the continental shelf. *Geological Survey of Canada Open File Report 1705,* Section 2, 33p.

DAVIDSON, S. and AMOS, C.L., 1985. A re-evaluation of SED1D and SED2D: Sediment transport models for the continental shelf. *Geological Survey of Canada Open File Report 1705,* Section 3, 54p.

DYER, K.R., 1980. Velocity profiles over a rippled bed and the threshold of movement of sand. *Estuarine and Coastal Marine Science,* 10, 181–199.

DYER, K.R., 1986. *Coastal and Estuarine Sediment Dynamics.* Chichester: Wiley-Interscience, 342p.

ENGELUND, F., and HANSEN, E., 1967. *A Monograph on Sediment Transport in Alluvial Streams.* Copenhagen, Denmark: Teknisk Vorlag, 62p.

EVERTS, C.H., 1973. Particle overpassing on flat granular boundaries. *Journal of Waterways, Harbours and Coastal Engineering Division,* 99, 425–438.

GIBBS, R.J.; MATTHEWS, M.D., and LINK, D.A., 1971. The relationship between sphere size and settling velocity. *Journal of Sedimentary Petrology,* 41(1), 7–18.

GILBERT, G.K., 1914. Transportation of debris by running water. *U.S. Geological Survey Professional Paper 86.*

GRACE, R.A., 1976. Near-bottom water motion under ocean waves. *Proceedings of the 15th Coastal Engineering Conference* (Honolulu), 3, 2371–2386.

GRANT, W.D. and GLENN, S.M., 1983. *Continental Shelf Bottom Boundary Layer Model.* Volume 1: Theoretical Model Development. Woods Hole: Woods Hole Oceanographic Institute, 163p.

GRANT, W.D. and MADSEN, S.M., 1982. Movable bed roughness in unsteady oscillatory flow. *Journal Geophysical Research,* 87(C1), 469–481.

GRANT, W.D. and MADSEN, O.S., 1979. Combined wave and current interaction with a rough bottom. *Journal Geophysical Research,* 84(4), 1797–1808.

GRANT, W.D. and MADSEN, O.S., 1978. Bottom friction under waves in the presence of a weak current. *National Oceanic and Atmospheric Administration Technical Memorandum ERL MESA-29,* 139p.

GROSS, T.F., WILLIAMS, A.J. and TERRAY, E.A., 1996? Bottom boundary layer spectral dissipation estimates in the presence of wave motions. *Continental Shelf Research,* 14, 1239–1256.

GUZA, R.T. and THORNTON, E.B., 1980. Local and shoaled comparisons of sea surface elevations, pressures, and velocities. *Journal of Geophysical Research,* 85(C3), 1524–1530.

HAMMOND, T.M. and COLLINS, M.B., 1979. On the threshold of transport of sand-sized sediment under the combined influence of unidirectional and oscillatory flow. *Sedimentology,* 26, 795–812.

HEATHERSHAW, A.D., 1981. Comparisons of measured and predicted sediment transport rates in tidal currents. *Marine Geology,* 42, 75–104.

HEFFLER D.E., 1984. RALPH—an instrument to monitor seabed sediments. Current Research, Part B. *Geological Survey of Canada Paper 84-1B,* pp. 47–52.

HODGINS, D.O.; DRAPEAU, G., and KING, L.H., 1986. Field measurements of sediment transport on the Scotian Shelf. Volume I the radio-isotope experiment. *Environmental Studies Revolving Funds Report 041,* Ottawa, 160p.

HODGINS, D.O.; HUNTLEY, D.A.; LIAM FINN, W.D.; LONG, B.; DRAPEAU, G., and BOWEN, A.J., 1986. Bottom sediment transport—present knowledge and industry needs. *Environmental Studies Revolving Funds Report 027,* Ottawa, 394p.

HODGINS, D.O. and SAYAO, O.J., 1986. Field measurements of sediment transport on the Scotian Shelf. Volume II boundary layer measurements and sand transport prediction. Ottawa: *Environmental Studies Revolving Funds Report 041,* 114p.

HUNTLEY, D.A., 1986. Physical concepts of sediment transport on continental shelves. *In:* HODGINS, D.O. (ed.), *Sediment Transport—Present Knowledge and Industry Needs.* Ottawa: Environmental Studies Revolving Funds Report 027, pp. 3–57.

HUNTLEY, D.A.; AMOS, C.L.; WILLIAMS, J.J., and HUMPHREY, J.D., 1991. Estimating bedload transport on continental shelves by observations of ripple migration—An assessment. *In:* SOULSBY, R. and BETESS, R. (eds.), *Euromech 262—Sand Transport in Rivers, Estuaries and the Sea.* Rotterdam: Balkema, pp. 17–24.

HUNTLEY D.A. and HAZEN, D.G., 1988. Sea bed stresses and combined wave and steady flow conditions on the Nova Scotia continental shelf; field measurements and predictions. *Journal of Physical Oceanography,* 18, 347–362.

INMAN, D.L. and BOWEN, A.J. 1963. Flume experiments on sand transport by waves and currents. *Proceedings 8th Conference Coastal Engineering* (ASCE, New York), pp. 137–150.

JONSSON, I.G., 1966. Wave boundary layers and friction factors. *Proceedings 10th Conference on Coastal Engineering.* New York: American Society of Civil Engineers, pp. 127–148.

KACHEL, N.B. and STERNBERG, R.W., 1971. Transport of bedload as ripples during an ebb current. *Marine Geology,* 10, 229–244.

KOMAR, P.D., 1976. Boundary layer flow under steady unidirectional currents. *In:* STANLEY, D.J. and SWIFT, D.J.P. (eds.). *Marine Sediment Transport and Environmental Management.* New York: Wiley, pp. 91–106.

KOMAR, P.D. and MILLER, M.C., 1975. Sediment threshold under

oscillatory waves. *Proceedings of 14th Coastal Engineering Conference.* (Copenhagen), pp. 756–775.

LANGHORNE, D.N., 1981. An evaluation of Bagnold's dimensionless coefficient of proportionality using measurements of sand wave movement. *Marine Geology,* 43, 49–64.

LANGHORNE, D.N., 1982. A study of the dynamics of a marine sandwave. *Sedimentology,* 29(4), 571–594.

LARSEN, L.H.; STERNBERG, R.W.; SHI, N.C.; MADSEN, M.A.H., and THOMAS, L., 1981. Field investigations of the threshold of grain motion by ocean waves and currents. *Marine Geology,* 42, 105–132.

LAVELLE, J.W.; SWIFT, D.J.P.; GADD, P.E.; STUBBLEFIELD, W.L.; CASE, F.N.; BRASHEAR, H.R., and HAFF, K.W., 1978. Fair weather and storm sand transport on the Long Island, New York, inner shelf. *Sedimentology,* 25, 823–842.

LEEDER, M.R., 1979. Bedload dynamics: Grain impacts, momentum transfer and derivation of a grain Froude number. *Earth Surface Processes,* 4, 1569–1588.

LEE, B.J., 1983. The relationship of sediment transport rates and paths to sandbanks in a tidally dominated area off the coast of East Anglia, U.K. *Sedimentology,* 30, 461–483.

LI, M.Z. and AMOS, C.L., 1997. SEDTRANS96: Upgrade and calibration of the GSC sediment transport model. *Geological Survey of Canada Open File 3512,* 140p.

LI, M.Z. and AMOS, C.L., 1995. SEDTRANS92: A sediment transport model for continental shelves. *Computers & Geosciences,* 21(4), 533–554.

LONGUET-HIGGINS, M.S., 1952. On the statistical distribution of the heights of sea waves. *Journal of Marine Research,* 11(3), 245–266.

MADSEN, O.S. and GRANT, W.D., 1976. *Sediment Transport in the Coastal Environment.* Cambridge: Massachusetts Institute of Technology, Department of Civil Engineering Report 209, 105p.

MARTEC LTD., 1982. *Sediment Transport on a Continental Shelf.* Consultant Report submitted to Geological Survey of Canada, Darmouth (DSS file # 10SC 23420-1-M571), 91p.

MARTEC LTD., 1983. A 2-D sediment transport model for continental shelves. *Geological Survey of Canada Open File Report 1705,* Section 1, 4.3p.

MARTEC LTD., 1986. The comparison between observed and predicted sediment transport for the radio-active sand tracer study and SED1D model upgrade. *Geological Survey of Canada Open File Report 1705,* section 5-9, F.3p.

MARTEC LTD., 1987. Upgrading of AGC sediment transport model. *Geological Survey of Canada Open File Report 1705,* Section 10, C.14p.

MICHE, R., 1944. Mouvements ondulatoires des mers en profendeur constante en decroissante. *Annales des Ponts et Chausees,* 25–78.

MILLER, M.C.; MCCAVE, I.N., and KOMAR, P.D., 1977. Threshold of sediment motion under unidirectional currents. *Sedimentology* 24: 507–527.

MOBIL OIL Canada Ltd. 1983. Venture development project environmental impact statement, volIIIb, biophysical assessment. Impact Statement submitted to Canadian Oil and Gas Lands Administration, Ottawa: 415p.

MOODY, J.A.; BUTMAN, B., and BOTHNER, M. H. 1987. Near-bottom suspended matter concentration on the continental shelf during storms: Estimates based on *in situ* observations of light transmission and a particle size dependent transmissometer calibration. Continental Shelf Research 7, 609–628.

NIEDORODA, A.W.; MA, C-M, MANGARELLA, P.A.; CROSS, R.A.; HUNTSMAN, S.R.; and TREADWELL, D. D. 1982. Measured and computed coastal ocean bedload transport. Proc. 18th Coastal Engineering Conference vol. 2. Publ. ASCE, New York: 1353–1368.

NIELSEN, P. 1979. Some basic concepts of wave sediment transport. Institute Hydrodynamics and Hydraulic Engineering, Technical University of Denmark Paper 20: 160p.

NIELSEN, P. 1986. Suspended sediment concentrations under waves. Coastal Engineering 10: 23–31.

NIELSEN, P. 1992. *Coastal Bottom Boundary Layers and Sediment Transport.* Singapore: Publ. World Scientific: 324p.

PATTIARATCHI, C.B. and COLLINS, M.B. 1984. Sediment transport under waves and currents: A case study from the northern Bristol Channel. *U.K. Marine Geology* 56, 27–40.

RUBIN, D.M. and MCCULLOCH, D.S. 1980. Single and superimposed bedforms: A synthesis of San Francisco Bay and flume observations. *Sedimentary Geology* 26, 207–231.

SAMAGA, B.R.; RAJU, K.G.R., and GARDE, R.J. 1986. Suspended load transport of sediment mixtures. Journal of Hydraulic Engineering 112(11): 1019–1035.

SINGLETON, R.C., 1969. An algorithm for computing the mixed radix fast Fourier transform. *IEEE Transaction Audio and Electro-Acoustics,* AU-17(2), 93–103.

SLEATH, J.F.A., 1984. *Sea Bed Mechanics.* New York: Wiley, 335p.

SMITH J.D., 1977. Modeling of sediment transport on continental shelves. *In:* O'BRIEN, J.J. and STEELE, J.H. (eds.). *The Sea,* New York: Wiley-Interscience, pp. 539–577.

SOULSBY, R.L., 1997. *Dynamics of Marine Sands. A Manual for Practical Applications.* HR Wallingford Report SR 466, 142p.

SOULSBY, R.L., 1983. The bottom boundary layer of shelf seas. *In:* JOHNS, B. (ed.). *Physical Oceanography of Coastal and Shelf Seas.* Amsterdam: Elsevier, pp. 189–266.

SOULSBY, R.L.; DAVIES, A.G., and WILKINSON, R.H., 1983. The detailed processes of sediment transport by tidal currents and by surface waves. *Institute of Oceanographic Sciences, Report, Tauton,* 152, 80p.

SOUTHGATE, H.N., 1987. A one-dimensional model of wave-current interaction. *Coastal Hydrodynamics.* New York: American Society of Civil Engineers, pp. 79–92.

SPIEGEL, M.R., 1961. *Theory and Problems of Statistics.* New York: McGraw-Hill, 359p.

SROKOSZ, M.A., 1987. Models of wave-current interaction. *Advances in Underwater Technology, Ocean Science and Offshore Engineering 12,* London: Graham and Trotman, pp. 313–325.

STERNBERG, R.W., 1967. Measurements of sediment movement and ripple migration in a shallow marine environment. *Marine Geology,* 5, 195–205.

STERNBERG, R.W., 1972. Predicting initial motion and bedload transport of sediment particles in the shallow marine environment. *In:* SWIFT, D.J.P., DUANE, D.B., and PILKEY, O.H. (eds.). *Shelf Sediment Transport, Process and Pattern.* Stroudsburg, Pennsylvania: Dowden, Hutchinson and Ross, pp. 61–83.

TERZAGHI, K. and PECK, R.B., 1967. *Soil Mechanics in Engineering Practice.* New York: Wiley, 729p.

THORN, M.F.C., 1979. The effects of waves on the tidal transport of sand. *Hydraulic Research Station Notes 21,* Wallingford, pp. 4–5.

VAN DEN BERG, J.H., 1987. Bedform migration and bed-load transport in some rivers and tidal environments. *Sedimentology,* 34(4), 681–698.

VAN RIJN, L.C., 1982. Equivalent roughness of alluvial bed. *Journal of Division of American Society of Civil Engineers,* 108(HY10), 1215–1218.

VINCENT, C.E. and DOWNING, A. 1994. Variability of suspended sand concentrations, transport and eddy diffusivity under non-breaking waves on the shoreface. *Continental Shelf Research,* 14, 223–250.

VINCENT, C.E.; YOUNG, R.A., and SWIFT, D.J.P., 1981. Bed-load transport under waves and currents. *Marine Geology,* 39, 71–80.

VINCENT, C.E.; YOUNG, R.A., and SWIFT, D.J.P., 1983. Sediment transport on the Long Island shoreface, North American Atlantic Shelf: Role of waves and currents in shoreface maintenance. *Continental Shelf Research,* 2, 163–181.

WHEATCROFT, R.A., 1994. Temporal variation in bed configuration and one-dimensional bottom roughness at the mid-shelf STRESS site. *Continental Shelf Research,* 14, 1167–1190.

WIBERG, P.L.; DRAKE, D.E., and CACCHIONE, D.A. 1994. Sediment resuspension and bed armouring during high bottom stress events on the northern California inner continental shelf: measurements and predictions. *Continental Shelf Research,* 14, 1191–1219.

WIBERG, P.L. and NELSON, J.M., 1992. Unidirectional flow over asymmetric and symmetric ripples. *Journal of Geophysical Research,* 97, 12,745–12,761.

WIBERG, P. and SMITH, J.D., 1983. A comparison of field data and theoretical models for wave-current interactions at the bed on the continental shelf. *Continental Shelf Research,* 2, 147–162.

WILLIS, D.H., 1979. Sediment load under waves and currents. *DME/NAE Quarterly Bulletin*, 3, 17p.
YALIN, M.S., 1977. *Mechanics of Sediment Transport.* Oxford: Pergamon, 298p.
YANG, C-S., 1986. On Bagnold's sediment transport equation in tidal marine environments and the practical definition of bedload. *Sedimentology,* 33(4), 465–486.
YOO, D., and O'CONNER, B.A., 1987. Bed friction model of wave-current interacted flow. *Coastal Hydrodynamics.* New York: American Society of Civil Engineers, pp. 93–106.

## NOTATION

| | |
|---|---|
| $A_b$ | maximum wave orbital amplitude (L) |
| $a_{md}$ | wave amplitude mean deviation |
| $a_{rms}$ | root-mean-square wave amplitude |
| $c_d$ | Soulsby's (1983) "unrippled bed" drag coefficient |
| $C_o$ | Bagnold's (1966) static volume concentration |
| d | water depth (L) |
| $d_o$ | maximum wave orbital diameter ($2A_b$) (L) |
| $d_r$ | ripple displacement (L) |
| $D_{50}$ | mean sediment grain diameter (L) |
| $f_c$ | pure current friction factor |
| $f_w$ | pure wave friction factor |
| $f_{cw}$ | current-enhanced wave friction factor |
| H | deep water wave height (L) |
| $H_b$ | breaker height (L) |
| $H_s$ | significant wave height (L) |
| K | Bagnold's (1963) efficiency term |
| $K_b$ | bed roughness height (L) |
| k | wave number ($T^{-1}$) |
| L | deep water wavelength (L) |
| $Q_s$ | sediment transport rate ($ML^{-1}T^{-1}$) |
| Re | Reynold's number |
| $U_1$ | mean current 1 m above the seabed ($LT^{-1}$) |
| $U_a$ | mean current at top of wave boundary layer ($LT^{-1}$), after Grant and Madsen (1979) |
| $U_b$ | maximum near-bed wave orbital velocity ($LT^{-1}$), after Grant and Madsen (1979) |
| $U_{cb}$ | critical current speed for sediment traction ($LT^{-1}$) |
| $U_{max}$ | maximum near-bed wave orbital velocity ($LT^{-1}$), after Miller *et al.* (1977) |
| $U_{md}$ | mean current mean deviation |
| $U_{cs}$ | critical current speed for sediment suspension ($LT^{-1}$) |
| $U_*$ | friction velocity ($LT^{-1}$) |
| T | wave period (T) |
| $W_s$ | grain settling velocity ($LT^{-1}$) |
| tan $\alpha$ | internal friction angle |
| $\eta$ | ripple height (L) |
| $\theta_w$ | wave Shields parameter |
| $\theta_c$ | current wave Shields parameter |
| $\theta_{cb}$ | critical Shields parameter for sediment traction |
| $\lambda$ | ripple wavelength (L) |
| $\mu$ | absolute viscosity of seawater ($ML^{-1}T^{-1}$) |
| $\upsilon$ | kinematic viscosity of seawater ($L^2T^{-1}$) |
| $\rho_s$ | density of sediment ($ML^{-3}$) |
| $\rho_f$ | density of seawater ($ML^{-3}$) |
| $\rho_b$ | dry bulk density of sediment ($ML^{-3}$) |
| $\sigma$ | coefficient of sediment sorting |
| $\tau_w$ | wave-induced bed shear stress ($ML^{-1}T^{-2}$) |
| $\tau_b$ | mean bed shear stress ($ML^{-1}T^{-2}$) |
| $\tau_{cb}$ | critical bed shear stress for traction ($ML^{-1}T^{-2}$) |
| $\tau_s$ | critical bed shear stress for suspension ($ML^{-1}T^{-2}$) |
| $\varphi_b$ | angle between waves and currents inside wave boundary layer |
| $\omega$ | wave number ($T^{-1}$) |
| ′ | denotes the skin friction component (no form drag) |